N73-15813

MSC-05161
SUPPLEMENT 3

NATIONAL AERONAUTICS AND SPACE ADMINISTRATION

# APOLLO 15 MISSION REPORT

## SUPPLEMENT 3

## ASCENT PROPULSION SYSTEM FINAL FLIGHT EVALUATION





MANNED SPACECRAFT CENTER
HOUSTON, TEXAS
SEPTEMBER 1972

MSC-05161
Supplement 3

# APOLLO 15 MISSION REPORT

## SUPPLEMENT 3

## ASCENT PROPULSION SYSTEM FINAL FLIGHT EVALUATION

PREPARED BY

TRW Systems

APPROVED BY

Owen G. Morris
Manager, Apollo Spacecraft Program

NATIONAL AERONAUTICS AND SPACE ADMINISTRATION
MANNED SPACECRAFT CENTER
HOUSTON, TEXAS
SEPTEMBER 1972

20029-H062-R0-00

PROJECT TECHNICAL REPORT

# APOLLO 15

# LM-10
# ASCENT PROPULSION SYSTEM
# FINAL FLIGHT EVALUATION

NAS 9-12330

MARCH 1972

Prepared for
NATIONAL AERONAUTICS AND SPACE ADMINISTRATION
MANNED SPACECRAFT CENTER
HOUSTON, TEXAS

Prepared by
Propulsion Systems Section
Applied Mechanics Department

20029-H062-R0-00

PROJECT TECHNICAL REPORT

# APOLLO 15

# LM-10
# ASCENT PROPULSION SYSTEM
# FINAL FLIGHT EVALUATION

NAS 9-12330

MARCH 1972

Prepared for
NATIONAL AERONAUTICS AND SPACE ADMINISTRATION
MANNED SPACECRAFT CENTER
HOUSTON, TEXAS


Prepared by
W. G. Griffin
Propulsion Systems Section
Applied Mechanics Department


NASA

Concurred by: Z. D. Kirkland, Head
Systems Analysis Section

Concurred by: R. E. Taylor, Manager
Ascent Propulsion Subsystem

Concurred by: C. W. Yodzis, Chief
Primary Propulsion Branch

TRW SYSTEMS

Approved by: R. J. Smith, Manager
Task E-99

Approved by: J. M. Richardson, Head
Propulsion Systems Section

Approved by: R. G. Payne, Manager
Applied Mechanics Department

CONTENTS



TABLES

CONTENTS (Continued)

ILLUSTRATIONS

# 1. PURPOSE AND SCOPE

The purpose of this report is to present the results of the postflight analysis of the Ascent Propulsion System (APS) performance during the Apollo 15 Mission. It is a supplement to the Apollo 15 Mission report. Determination of the APS steady-state performance under actual flight environmental conditions was the primary objective of the analysis. Included in the report are such information as required to provide a comprehensive description of APS performance during the Apollo 15 Mission.

Major additions and changes to the preliminary results presented in the mission report (Reference 1) are listed below.

1) Calculated performance values for the APS lunar liftoff burn.
2) Discussion of analysis techniques, problems and assumptions.
3) Comparision of postflight analysis and preflight prediction.
4) Reaction Control System (RCS) duty cycle included in the APS performance analysis.
5) Transient performance analysis.
6) The APS propellant consumption values presented in the preliminary postflight evaluation have been revised as shown in Table 2.

## 2. SUMMARY

The duty cycle for the LM-10 APS consisted of two firings, an ascent stage liftoff from the lunar surface and the Terminal Phase Initiation (TPI) burn. APS performance for the first firing was evaluated and found to be satisfactory. No propulsion data were received from the second APS burn; however, all indications were that the burn was nominal.

Engine ignition for the APS lunar liftoff burn occurred at the Apollo elasped time (AET) of 171:37:23.2 (hours:minutes:seconds). Burn duration was 430.9 seconds.

Average steady-state engine performance parameters for the burn are as follows:

Thrust - 3540 lbf

Isp - 311.7 sec

Mixture Ratio - 1.610

All performance parameters were well within their LM-10 3-sigma limits. Calculated throat erosion at engine cutoff for the LM-10 APS was approximately 3 percent greater than predicted.

## 3. INTRODUCTION

The APS duty cycle for the Apollo 15 Mission consisted of a lunar liftoff burn and a Terminal Phase Initiation (TPI) burn. Total burn duration for the two firings was 433.5 seconds. The Apollo 15/LM-10/APS was equipped with Rocketdyne Engine S/N 0014C. APS engine performance characterization equations used in preflight analyses and as a basis for the postflight evaluation are found in Reference 2. Engine acceptance test data used in the determination of performance are from Reference 3. Physical characteristics of the engine and feed system are presented in Table 1.

Ignition time for the initial APS firing was 171:37:23.2 AET. Engine cutoff was commanded at 171:44:34.1 AET for an APS burn duration of 430.9 seconds. Loss of signal (LOS) occurred following engine shutdown for the lunar liftoff burn at approximately 171:51 AET as the vehicle went behind the moon. The second APS burn was the 2.6 Second Terminal Phase (TPI) maneuver. APS engine ignition time for the TPI manuever was 172:29:40 AET, approximately 38 minutes after LOS. Exact data concerning ascent stage main engine ignition and cutoff times and the assoicated velocity changes are shown below:

| Burn | Ignition Hr:min:sec. | Engine Cutoff Hr:min:sec. | Burn Time Seconds | Velocity (1) Change, ft/sec |
|---|---|---|---|---|
| Lunar Liftoff | 171:37:23.2 | 171:44:34.1 | 430.9 | 6059 |
| TPI | 172:29:40.0 | 172:29:42.6 | 2.6 | 72.7 |

(1) Reference 1

## 4. STEADY-STATE PERFORMANCE ANALYSIS

### Analysis Technique

Determination of APS steady-state performance during the lunar orbit insertion burn was the primary objective of the LM-10 postflight analysis. The insertion burn duration was 430.9 seconds, engine on to engine off command. In addition to the orbital insertion maneuver the APS was used to perform the Terminal Phase Initiation (TPI) burn. Burn duration for TPI was approximately 2.6 seconds. No propulsion system telemetry data are available from the TPI burn since the spacecraft was behind the moon.

The APS postflight analysis was conducted using the Apollo Propulsion Analysis Program (PAP) as the primary computational tool. Additionally, the Ascent Propulsion Subsystem Mixture Ratio Program (MRAPS) was used in an iterative technique with PAP to determine the vehicle propellant mixture ratio. Reference 4 presents a detailed explanation of the operation of the MRAPS program and the underlying theory which it implements.

An initial estimate of the ascent stage weight at lunar liftoff of 10915 lbm was obtained from Reference 5. Ascent stage damp weight (total spacecraft weight less APS propellants) was considered to be constant throughout the firing except for a 0.03 lbm/sec overboard flowrate which accounts for ablative nozzle erosion.

RCS propellant usage and thrust histories were obtained from an analysis of the RCS bi-level measurements. Approximately 95 percent of the RCS consumption during the ascent burn was from the APS tanks. The remaining 5 percent of the RCS usage, ~3 lbm, was from the RCS tanks following the closing of the APS/RCS interconnect valves. Table 2 presents a summary of propellant usage, including RCS consumption, from the APS tanks during the ascent burn. Propellant densities used in the program were based on equations from Reference 6, adjusted by measured density data for the LM-10 flight given in the Spacecraft Operational Data Book (SODB), Reference 7. Oxidizer and fuel temperatures were taken from flight measurement data and were 68.25°F and 69.75°F, respectively. These temperatures were considered to be constant throughout the segment of burn analyzed. The following flight measurement data were used in the analysis of the LM-10 APS burn: engine chamber pressure, engine interface pressures, vehicle thrust acceleration, propellant tank bulk temperatures, helium regulator outlet pressures, engine on-off commands, helium tank pressure measurements, and RCS thruster solenoid bi-level measurements. Measurement numbers and data pertinent to the above measurements, with the exception of RCS bi-levels, are given in Table 3. Plots of measurement data versus time are presented in the appendix to this report.

## Flight Data Analysis and Results

A 400-second segment of the APS lunar liftoff burn was selected to be analyzed for the purpose of determining steady-state performance. The segment of the burn analyzed begins at 171:37:35.0 AET, 11.8 seconds after ignition, and ends at 171:44:15.0 AET, 19.1 seconds prior to cutoff. The periods immediately following ignition and immediately prior to engine cutoff are not included in order to minimize any errors resulting from data filtering spans which included the start and shutdown transients. APS engine propellant comsumption during the burn is presented in Table 2. Propellant consumption from engine on command to the start of the steady-state analysis segment and from the end of the steady-state analysis to the beginning of chamber pressure decay was extrapolated from steady-state analysis results.

The primary engine performance determinations made during the LM-10 postflight analysis are as follows: All average values are over the 400-second period of steady-state analysis.

1) Average APS specific impulse was 311.7 seconds.

2) Average APS mixture ratio was determined to be 1.610.

3) Average APS thrust was 3540 lbf.

4) Engine throat erosion was 3 percent greater than predicted at 400 seconds from ignition.

An extrapolation of the APS steady-state analysis to include the entire burn, with the exception of ignition and shutdown transients, resulted in an average specific impulse, thrust, and mixture ratio of approximately the same values as the 400 second burn segment. LM-10 APS performance was greater than predicted with the average engine specific impulse exceeding the predicted average value by 1.7 seconds.

The general solution approach used in the LM-10 flight evaluation was to calculate the vehicle weight (including propellant loads) for the beginning of the burn segment used to analyze steady-state performance and then allow the PAP to vary this weight and other selected performance parameters (state variables) in order to achieve an acceptable data match. The PAP simulations were made using the previously discussed APS engine characterization model driven by engine interface pressures. Raw flight interface pressure measurement data were first filtered with a sliding arc filter and then, because of excessive distortion, these data were further smoothed using a fifth degree curve fit.

Simulation of RCS activity was accomplished with a model that was developed from individual thruster "on" time. This technique has been used on all preceding APS reconstructions and is fully discussed in Reference 8.

Initial PAP simulation results based on the input data outlined in the beginning of this section indicated the predicted throat erosion was less than that required to match flight data. A revised throat erosion curve was calculated using the partial derivatives of throat area with respect to acceleration. The revision of the throat area curve included increasing the initial value to 16.432 $in^2$, about 0.3 percent larger than the preflight value. This technique has been used during previous APS postflight reconstructions and has yielded good results. The inclusion of this calculated throat area curve in the analysis program resulted in an excellent acceleration match with a near zero mean and no significant slope. The derived throat erosion was 3 percent greater than predicted at approximately 400 seconds after ignition. Figure 1 shows the calculated throat area curve in comparison with the predicted curve for LM-10.

An APS chamber pressure error model was derived from postflight data (Reference 9). In order to compensate for a suspected drift in the APS chamber pressure measurement (GP 2010), this model was used for the first time in the LM-10 APS postflight analysis. The comparison of reconstructed values to chamber pressure flight data achieved using the error model was good. The use of the error model allows the uncertainty associated with the chamber pressure measurement to be significantly reduced thus decreasing the overall uncertainty on the final minimum variance solution. A small ($\sim$.1 psia) chamber pressure measurement bias was determined by the final PAP solution. The residual match shown in Figure 3 incorporates both this bias and the previously discussed drift model.

Interface pressure measurement biases of approximately -2.0[1] psia and -.7[1] psia for oxidizer and fuel, respectively, were determined from the PAP results. It was noted during the flight that oxidizer interface pressure seemed to be lower than expected. These biases are well within the measurement accuracy for both the oxidizer (GP 1503) and fuel (GP 1501) interface pressure measurements.

A vehicle weight reduction of 17 lbm was determined from the PAP reconstruction. The best estimate of total ascent stage weight at lunar liftoff is 10898 lbm.

The principal indicator of the accuracy of the postflight reconstruction is the matching of calculated and measured acceleration data. A measure of the quality of the match is given by the residual slope and intercept data as shown in Figure 2. These data represent the ordinate intercept and the slope of a linear fit to the residual data. The closer both these numbers are to zero, the more accurate is the match. The acceleration match achieved with the LM-10 postflight reconstruction was very good. The LM-10 flight reconstruction was, by all indications, an accurate simulation of actual flight performance.

Figures 2 through 9 shows the principal performance parameters associated with the LM-10 postflight analysis. Four flight measurements were used as time varying input to the Propulsion Analysis Program. Two of these measurements, fuel and oxidizer interface pressure, were used as program drivers. The other two, acceleration and chamber pressure,

[1]As a convention in this report, a negative bias indicates that measured data was reading less than its true value.

were compared to calculated values by the program's minumim variance technique. The acceleration and chamber pressure measurements along with their residuals (measured data minus calculated) are presented in Figures 2 and 3 respectively. Figures 4 and 5 contain oxidizer and fuel interface pressure measurement data (after smoothing of the raw data), the curve fits of these data input to the Apollo Propulsion Analysis Program, and the residuals between the flight data and the calculated interface pressures. Calculated steady-state values for thrust, specific impulse, and oxidizer and fuel flowrates are shown in Figures 6-9.

## Comparison with Preflight Performance Prediction

Predicted performance of the LM-10 APS is presented in Reference 10. The intention of the preflight performance prediction was to simulate APS performance under flight environmental conditions for the Mission J-1 duty cycle. No attempt was made in the preflight prediction to simulate RCS operation.

Table 4 presents a summary of actual and predicted APS performance during the ascent burn. Engine specific impulse determined by the postflight reconstruction is greater than had been predicted but is still well within the 3-sigma limits of ±3.5 seconds presented in Reference 10. Comparisons of predicted and reconstructed values for specific impulse, thrust, and mixture ratio are presented in Figure 10 along with related 3-sigma dispersions. The variations in flight specific impulse, thrust and mixture ratio were within their respective 3-sigma dispersions.

## Engine Performance at Standard Interface Conditions

Expected APS engine flight performance was based on an engine characterization which utilized data obtained during engine and injector acceptance tests. In order to allow actual engine performance variations to be separated from variations induced by feed system, pressurization system, and propellant temperature variations, the acceptance test data are adjusted to a set of standard interface conditions; thereby providing a common basis for comparison. Standard interface conditions are as follows:

| | |
|---|---|
| Oxidizer interface pressure, psia | 170. |
| Fuel interface pressure, psia | 170. |
| Oxidizer interface temperature, °F | 70. |
| Fuel interface temperature, °F | 70. |
| Oxidizer density, $lbm/ft^3$ | 90.21 |
| Fuel density, $lbm/ft^3$ | 56.39 |
| Thrust acceleration, lbf/lbm | 1. |
| Throat area, $in^2$ | 16.48 |

Analysis results (at 13 seconds from ignition) for the ascent burn corrected to standard interface conditions and compared to acceptance test values are shown below:

| | Acceptance Test Date | Flight Analysis Results | % Difference |
|---|---|---|---|
| Thrust, lbf | 3501. | 3538. | 1% |
| Specific Impulse, $\frac{\text{lbf-sec}}{\text{lbm}}$ | 310.0 | 312.1 | 0.7% |
| Propellant Mixture Ratio | 1.597 | 1.597 | 0% |

Reduction of engine performance to standard interface conditions and comparison with acceptance test values shows good agreement with the largest difference being in the engine thrust. All differences are within two standard deviations of acceptance test values.

## 5. PRESSURIZATION SYSTEM

### Helium Utilization

The helium storage tanks were loaded to a nominal 13.2 lbm. There was no indication of leakage from the helium bottles during the mission and calculated usage agrees well with analytical predictions.

### Helium Regulator Performance

Helium regulator performance was approximately as predicted. The Class I primary regulator controlled helium flow throughout the burn. No significant oscillations in regulator outlet pressure were noted.

### Oxidizer Interface Pressure During Coast

A lower than expected (~3 psi) APS oxidizer interface pressure was noted during the translunar coast phase of the Apollo 15 Mission. However, the negative oxidizer interface pressure measurement bias previously discussed would account for 2 psi of the difference. Furthermore, the longer period from launch to pre-firing pressurization, i.e., 171 hours as opposed to 140 hours for LM-6 and LM-8 could account for an additional difference. The observed pressure difference is, therefore, not believed to be significant.

### Helium Manifold Pressure During Coast

A greater than expected pressure decay rate in the helium manifold was noted during the Apollo 15 translunar coast. The decay rate decreased as the flight progressed. A pressure of 10 psia is required in the helium manifold prior to APS final pressurization in order to verify the integrity of the helium manifold. The helium manifold pressure, as measured by the helium regulator outlet pressure (GP 0025) measurement was approximately

54 psia just prior to final pressurization. It was subsequently determined that the most likely source of leakage was the helium solenoid valves. These valves have been changed on LM-11 and no subsequent difficulties are expected.

## 6. PROPELLANT LOADING AND USAGE

APS propellant loads for the LM-10 Mission were 3225.6 lbm of oxidizer and 2011.4 lbm of fuel. Of these amounts 36.0 lbm of oxidizer and 15.9 lbm of fuel are considered to be unusable or consumed during transient engine operation. The amounts of nominally deliverable propellants are, therefore, 3189.6 lbm and 1995.5 lbm for oxidizer and fuel, respectively. Propellant density samples taken at the time of loading showed an oxidizer density of 1.4819 gm/cc at 4°C and a fuel density of 0.8979 gm/cc at 25°C. Both densities were at a pressure of one atmosphere.

Since all RCS propellant usage was from the RCS tanks prior to lunar liftoff, the APS propellant loads at APS ignition were 3225.6 lbm of oxidizer and 2011.4 lbm of fuel. Except for the last 20 seconds of burn, all RCS consumption during the ascent burn was through the APS/RCS interconnect. Total propellant usage from the APS tanks is presented in Table 2. The APS consumption during the lunar liftoff burn was 2978 lbm, oxidizer and 1855 lbm, fuel. Total RCS consumption, through the APS/RCS interconnect,during the APS first burn was 63 lbm. The TPI maneuver consumed as estimated 19 lbm of oxidizer and 12 lbm of fuel. A total of 186 lbm of oxidizer and 124 lbm of fuel remained onboard at APS second burn cutoff.

# 7. ENGINE TRANSIENT ANALYSIS

An analysis of the start and shutdown transients was performed with the primary intention of determining transient total impulse. Figures 11 and 12 are traces of engine chamber pressure, measurement GP2010, during start and shutdown of the lunar liftoff burn, repectively. No data were available from the TPI burn.

The time from ignition signal to 90 percent steady-state thrust was 0.345 seconds, well within the specification limit for unprimed starts of 0.450 seconds. Total start transient impulse was 27 lbf-sec. The chamber pressure overshoot exceeded the upper limit of the measurement range (150 psia); however, there were no indications of rough combustion or other abnormal performance.

Total impulse from engine cutoff signal to 10 percent thrust was 300 lbf-sec. Time from cutoff signal to 10 percent thrust was 0.19 seconds which is within the revised specification limit of 0.500 seconds (Reference 11).

# 8. CONCLUSIONS

The LM-10 APS flight reconstruction showed the APS performance to be satisfactory. No malfunctions or anomalies with possible impact on future flights were noted.

A statistical study of the differences between APS predicted and post-flight reconstructed specific impulse is contained in Reference 9. The results of the LM-10/APS analysis were added to the existing data shown in Reference 9, and from a study (Reference 12) of the expanded data set it is concluded that no change in the APS specific impulse prediction techniques are warranted at this time. This result will be verified by incorporating the results of future APS flight analyses as they become available.

REFERENCES

1. NASA Document, MSC-05161, "Apollo 15 Mission Report," December 1971.

2. North American Rockwell Corporation Document No. PAR 8114-4102, "Lunar Module Ascent Engine Performance Characterization," T. A. Clemmer, 10 July 1968.

3. Rocketdyne Engine Log Book, "Acceptance Test Data Package for Rocket Engine Assembly - Ascent LM - Part No. RS000580-001-04, Serial No. 0014," 8 July 1969.

4. Boeing Report D2-118346-1, "Computer Program Manual Ascent Propulsion Subsystem Mixture Ratio by the Center of Mass Method," 28 August 1970.

5. TRW IOC 71.6522:2.03, "Apollo 15 Postflight Mass Properties," C. A. Anderson to B. R. Ellison, 2 September 1971.

6. NASA Memorandum EP-23-10-69, from EP2/ Head Development Section to EP2/ Chief, Primary Propulsion Branch, "Propellant Densities ($N_2O_4$ and A-50)," 18 February 1969

7. Spacecraft Operational Data Book, SNA-8-D-027 (III), Rev. 3, Vol. III, Amendment 110.

8. TRW Report 17618-H146-R0-00, "Apollo 14/LM-8 Ascent Propulsion System Final Flight Evaluation," September 1971.

9. TRW IOC 71.4915:2.47, "Ascent Propulsion System (APS) Characterization," W. Griffin to E-99 File, 2 November 1971.

10. TRW Report 17618-H146-R0-00, "Apollo Mission J1/LM-10/APS Preflight Performance Report," May 1971.

11. LTX-965-219, "P.O. 6-20900-C, LM Ascent Engine, LVC 275-0050051A," 2 July 1969.

12. TRW IOC 72.4910.41-31, "APS Specific Impulse Characterization Study," W. G. Griffin to E-99 File, 1 March 1972.

TABLE 1. LM-10/APS ENGINE AND FEED SYSTEM PHYSICAL CHARACTERISTICS

| | |
|---|---|
| <u>Engine</u>[1] | |
| Engine No. | Rocketdyne S/N 0014C |
| Injector No. | Rocketdyne S/N 4097734 |
| Initial Chamber Throat Area ($in^2$) | 16.378[4] |
| Nozzle Exit Area ($in^2$) | 749.508 |
| Initial Expansion Ratio | 45.763 |
| Injector Resistance ($lbf\text{-}sec^2/lbm\text{-}ft^5$)@ time zero and 70°F | |
| Oxidizer | 12420.7 |
| Fuel | 19886.7 |
| <u>Feed System</u> | |
| Total Volume (Pressurized, Check Valves to engine interface)($ft^3$)[2] | |
| Oxidizer | 36.95 |
| Fuel | 37.00 |
| Resistance, Tank Bottom to Engine Interface ($lbf\text{-}sec^2/lbm\text{-}ft^5$) at 70°F[3] | |
| Oxidizer | 2459.52 |
| Fuel | 4065.12 |

(1) Rocketdyne Log Book, "Acceptance Test Data Package for Rocket Engine Assembly-Ascent LM-Part No. RS000580-001-04, Serial No. 0014," 8 July 1969 .

(2) NASA Memornadum EP23-46-69, "Propellant Load Parameters for the DPS and APS of LM-5 through LM-9 and the Estimated Parameters for LM-10 and Subsequent," from EP/Chief, Propulsion and Power Division to PD/Chief, Systems Engineering Division.

(3) GAC Memorandum LMO-271-844, "A/S Hydraulic Resistance LM 7, 8, 9," W. Salter, 6 December 1969.

(4) The initial throat area determined from postflight reconstruction was 16.432 $in^2$.

TABLE 2. PROPELLANT CONSUMPTION FROM APS TANKS

| | Oxidizer | Fuel |
|---|---|---|
| Propellant Loaded - lbm | 3225.6 | 2011.4 |
| Consumed During Lunar Liftoff Burn - lbm | | |
| APS | 2978.3 | 1854.8 |
| RCS | 42.0 | 21.0 |
| Total | 3020.3 | 1875.8 |
| Total Propellant Remaining - lbm | 205.3 | 135.6 |
| Consumed During TPI Burn - lbm | | |
| APS | 19.3 | 11.5 |
| Total Propellant Remaining - lbm | 186.0 | 124.1 |

TABLE 3. FLIGHT DATA USED IN STEADY-STATE ANALYSIS

| Measurement Number | Description | Range | Sample Rate Sample/sec |
|---|---|---|---|
| GP2010P | Pressure, Thrust Chamber | 0-150 psia | 200 |
| GP1503P | Pressure, Engine Oxidizer Interface | 0-250 psia | 1 |
| GP1501P | Pressure, Engine Fuel Interface | 0-250 psia | 1 |
| GP0025P | Pressure, Regulator Outlet Manifold | 0-300 psia | 1 |
| GP0018P | Pressure, Regulator Outlet Manifold | 0-300 psia | 1 |
| GP1218T | Temperature, Oxidizer Tank Bulk | 20-120°F | 1 |
| GP0718T | Temperature, Fuel Tank Bulk | 20-120°F | 1 |
| GH1260X | Ascent Engine On/Off | Off-On | 50 |
| GP0001P | Pressure, Helium Supply Tank No. 1 | 0-4000 | 1 |
| GP0002P | Pressure, Helium Supply Tank No. 2 | 0-4000 | 1 |
| GP0041P | Pressure, Helium Supply Tank No. 1 | 0-4000 | 10 |
| GP0042P | Pressure, Helium Supply Tank No. 2 | 0-4000 | 10 |
| CG0001X* | PGNS Downlink Data | Digital Code | 50 |

*Acceleration determined from PIPA data.

TABLE 4. LM-10 APS STEADY-STATE PERFORMANCE

| PARAMETER | 20 sec After Ignition | | | 200 sec After Ignition | | | 400 sec After Ignition | | |
|---|---|---|---|---|---|---|---|---|---|
| | Pred. (a) | Reconstructed(b) | Measured(c) | Pred.(a) | Reconstructed(b) | Measured(c) | Pred.(a) | Reconstructed(b) | Measured (c) |
| Regulator Outlet Pressure, psia | 184. | --- | 183.8 | 184. | --- | 183.8 | 184. | --- | 182.7 |
| Oxidizer Bulk Temperature °F | 70.0 | --- | 68.2 | 69.7 | --- | 68.2 | 69.0 | --- | 68.2 |
| Fuel Bulk Temperature °F | 70.0 | --- | 69.8 | 69.9 | --- | 69.8 | 69.8 | --- | 69.8 |
| Oxidizer Interface Pressure, psia | 170.8 | 170.7 | 168.3 | 170.7 | 170.1 | 168.2 | 170.0 | 168.8 | 166.4 |
| Fuel Interface Pressure, psia | 170.4 | 170.0 | 169.1 | 170.3 | 169.2 | 168.4 | 169.7 | 169.0 | 167.2 |
| Engine Chamber Pressure, psia | 123.9 | 123.6 | 123.8 | 124.3 | 123.0 | 123.8 | 123.7 | 120.9 | 122.4 |
| Mixture Ratio | 1.605 | 1.613 | --- | 1.600 | 1.611 | --- | 1.597 | 1.606 | --- |
| Thrust, lbf | 3515. | 3544. | --- | 3487. | 3535. | --- | 3484. | 3544. | --- |
| Specific Impulse, sec | 310.0 | 312.1 | --- | 310.2 | 312.0 | --- | 309.6 | 310.9 | --- |

(a) Preflight prediction based on acceptance test data and assuming nominal system performance.

(b) Reconstruction minimum variance technique.

(c) Smoothed flight data without biases determined by postflight analysis.

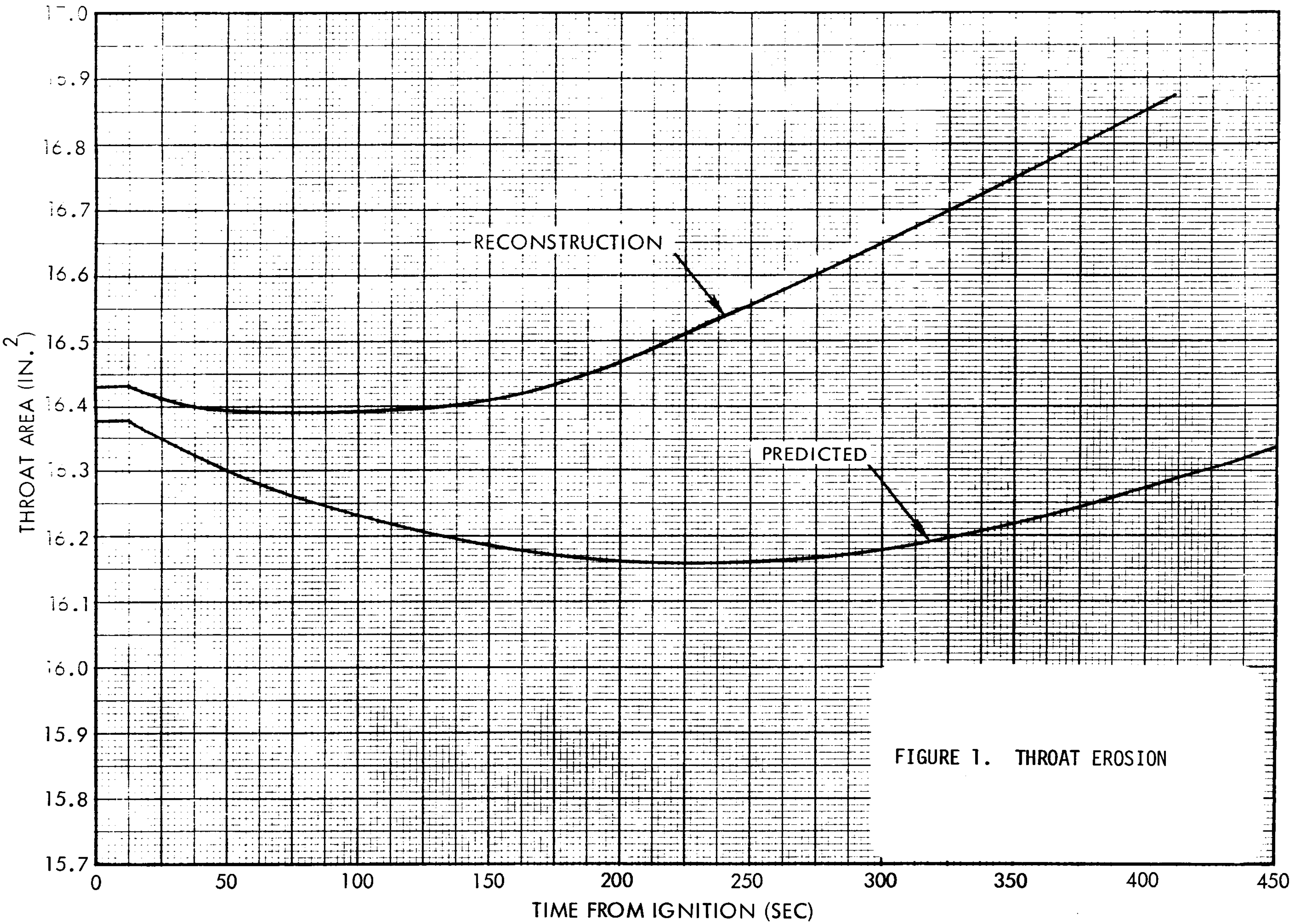


FIGURE 1. THROAT EROSION

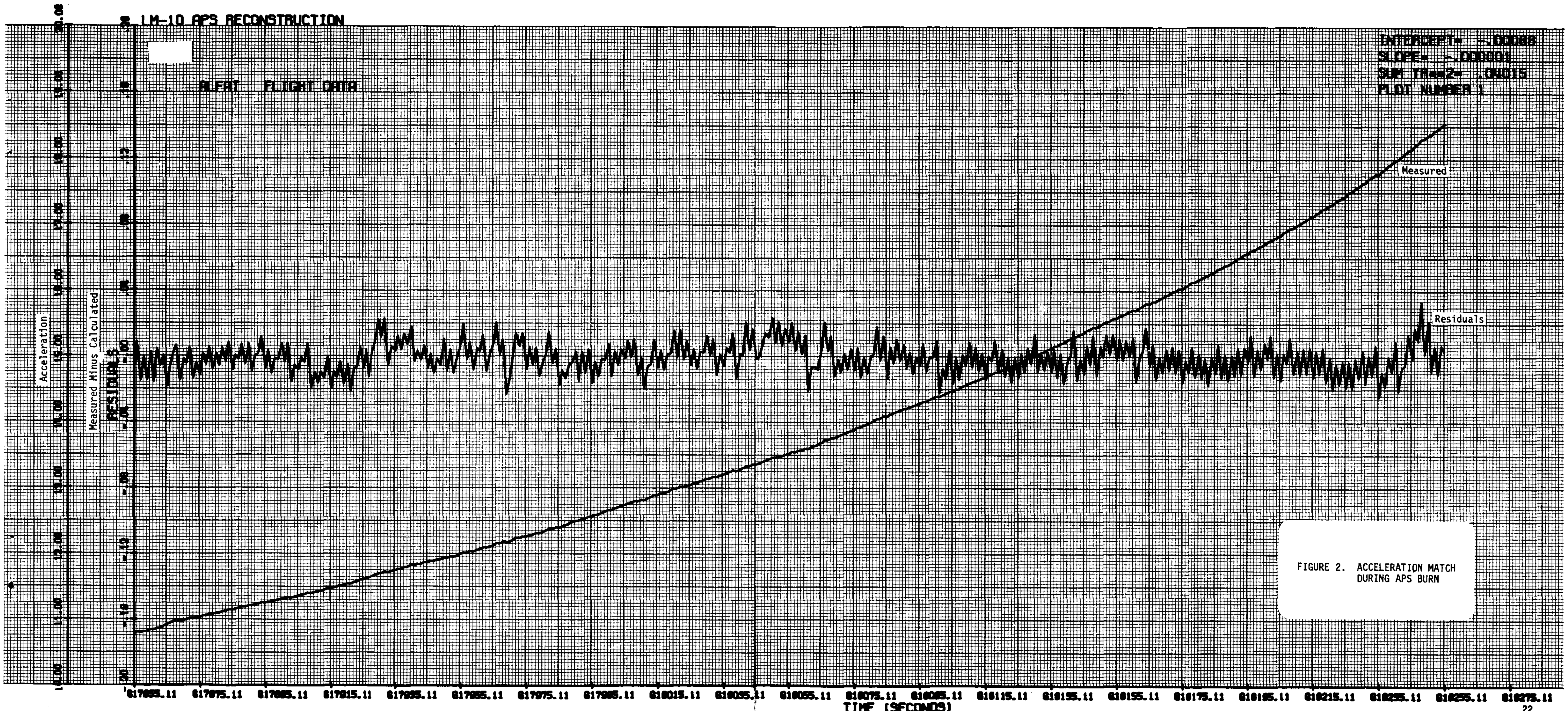


FIGURE 2. ACCELERATION MATCH DURING APS BURN

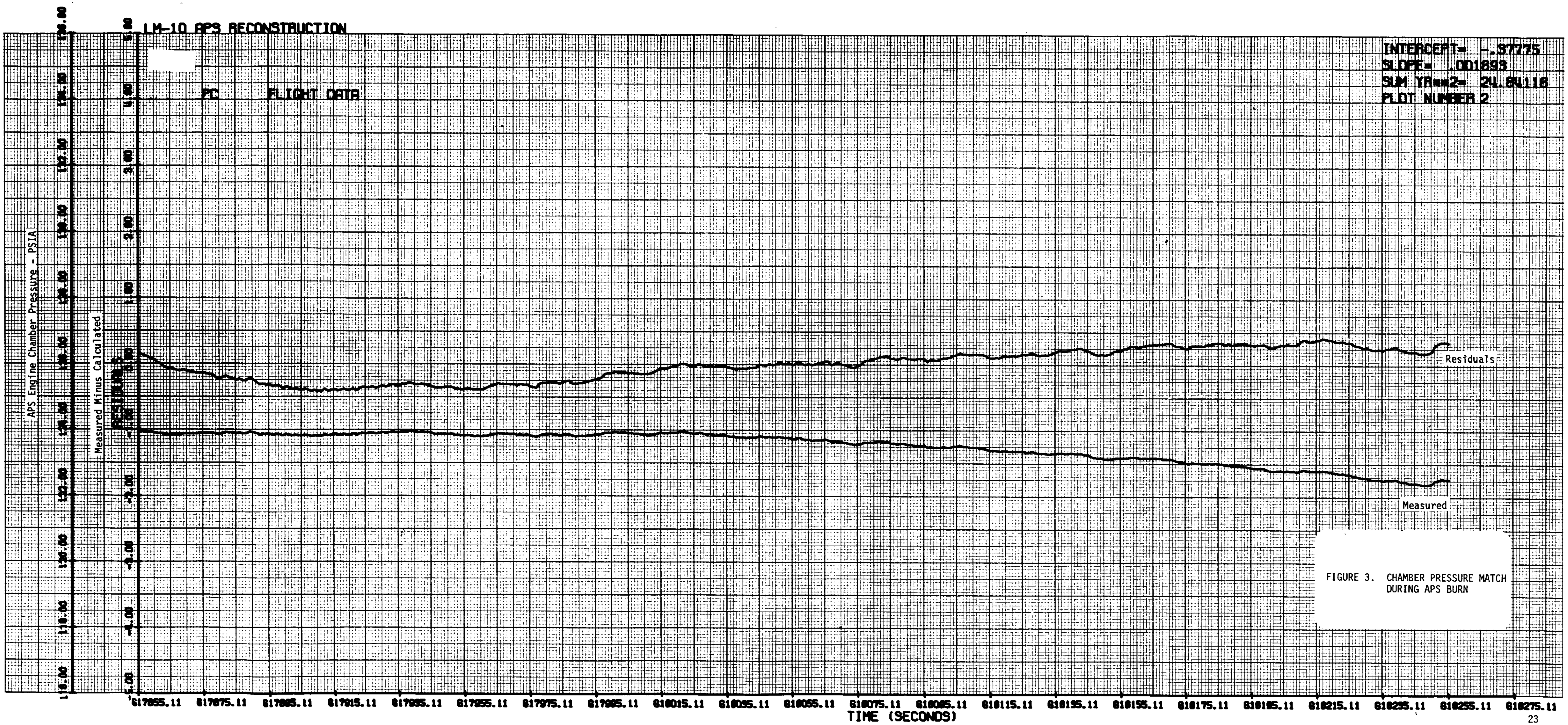


FIGURE 3. CHAMBER PRESSURE MATCH DURING APS BURN

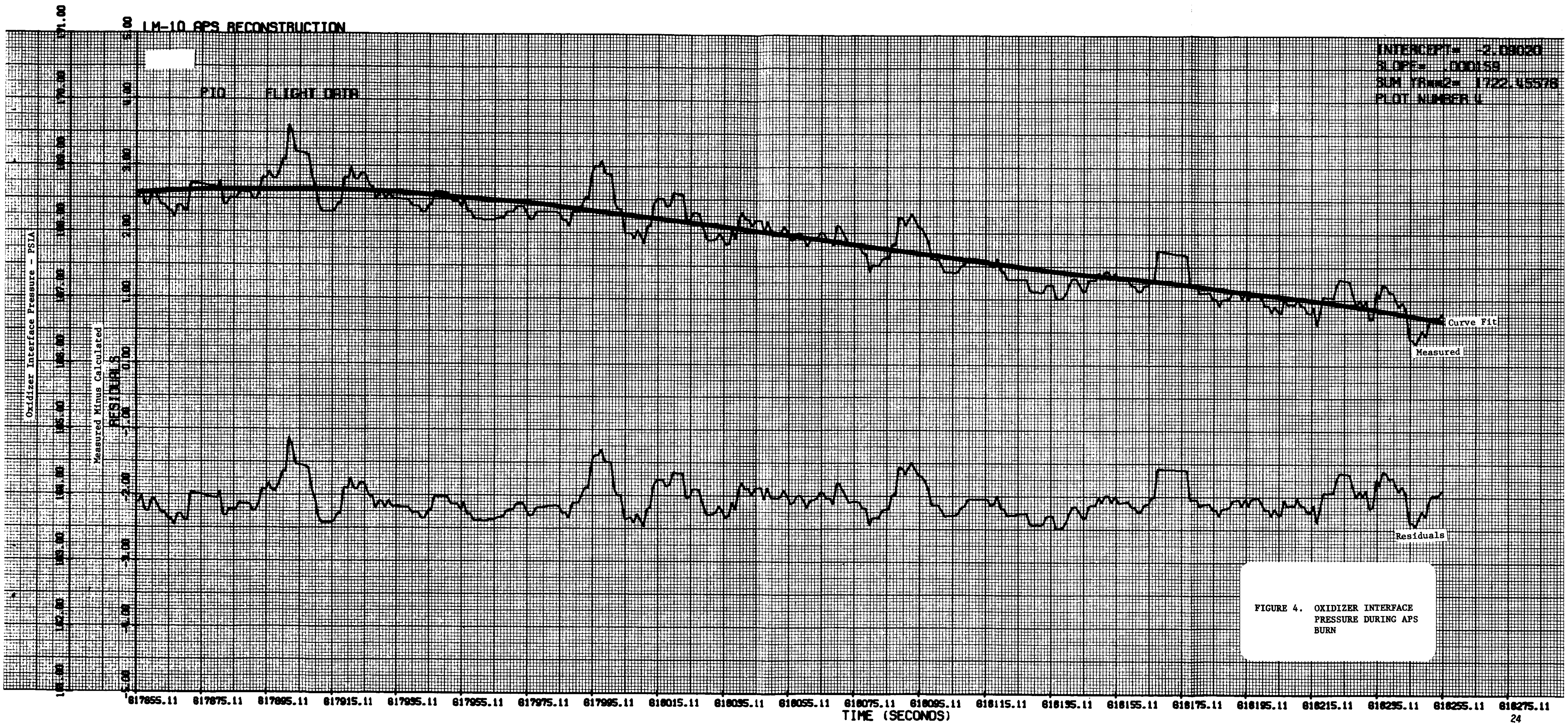


FIGURE 4. OXIDIZER INTERFACE PRESSURE DURING APS BURN

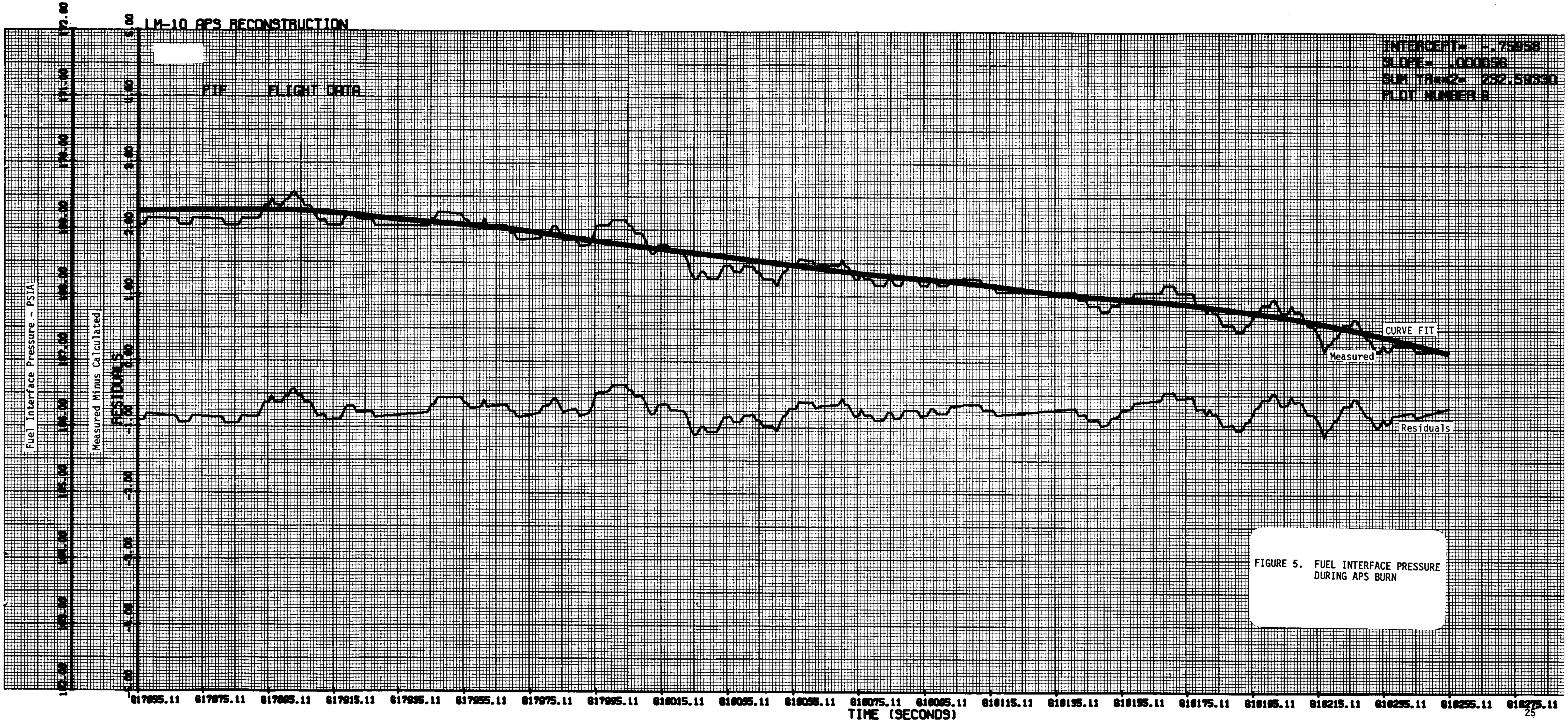


FIGURE 5. FUEL INTERFACE PRESSURE DURING APS BURN

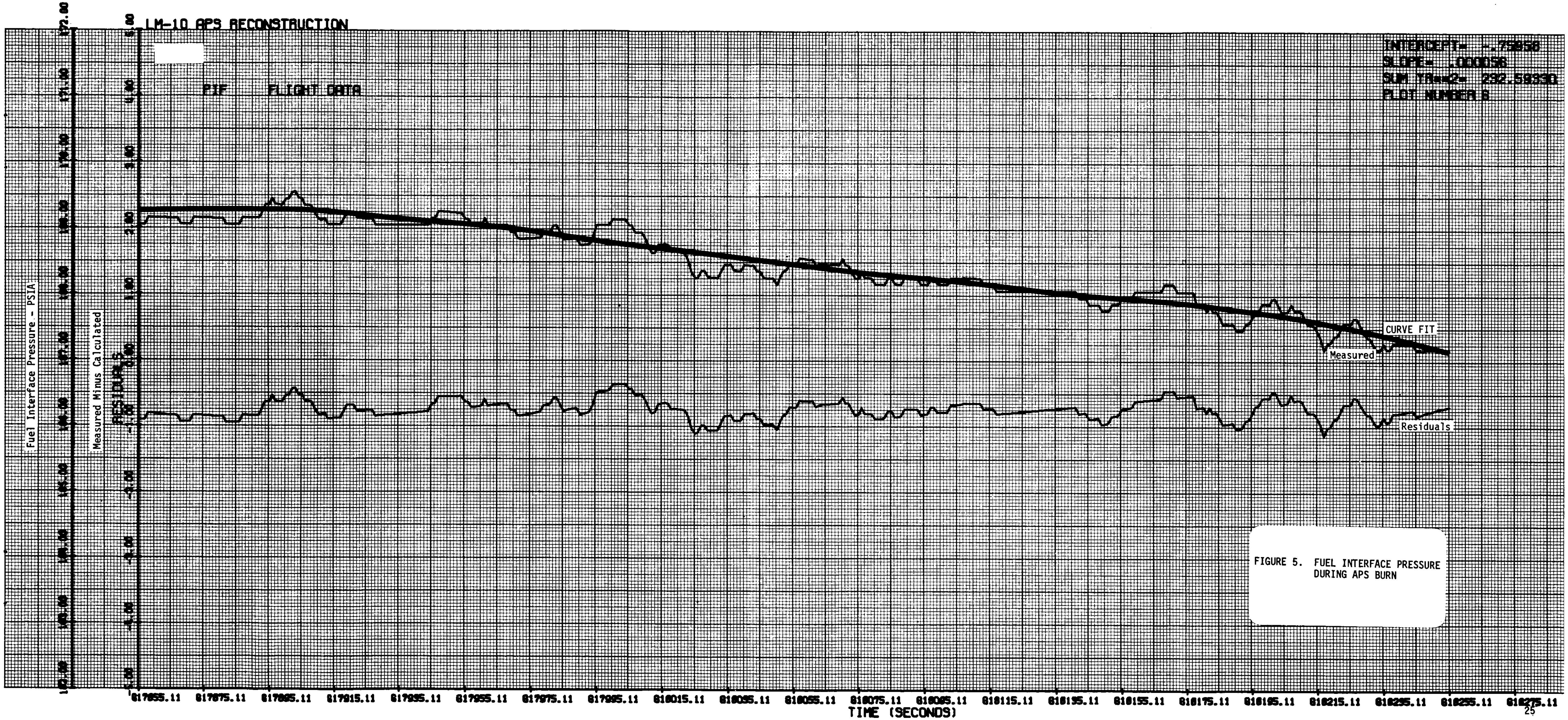


FIGURE 5. FUEL INTERFACE PRESSURE DURING APS BURN

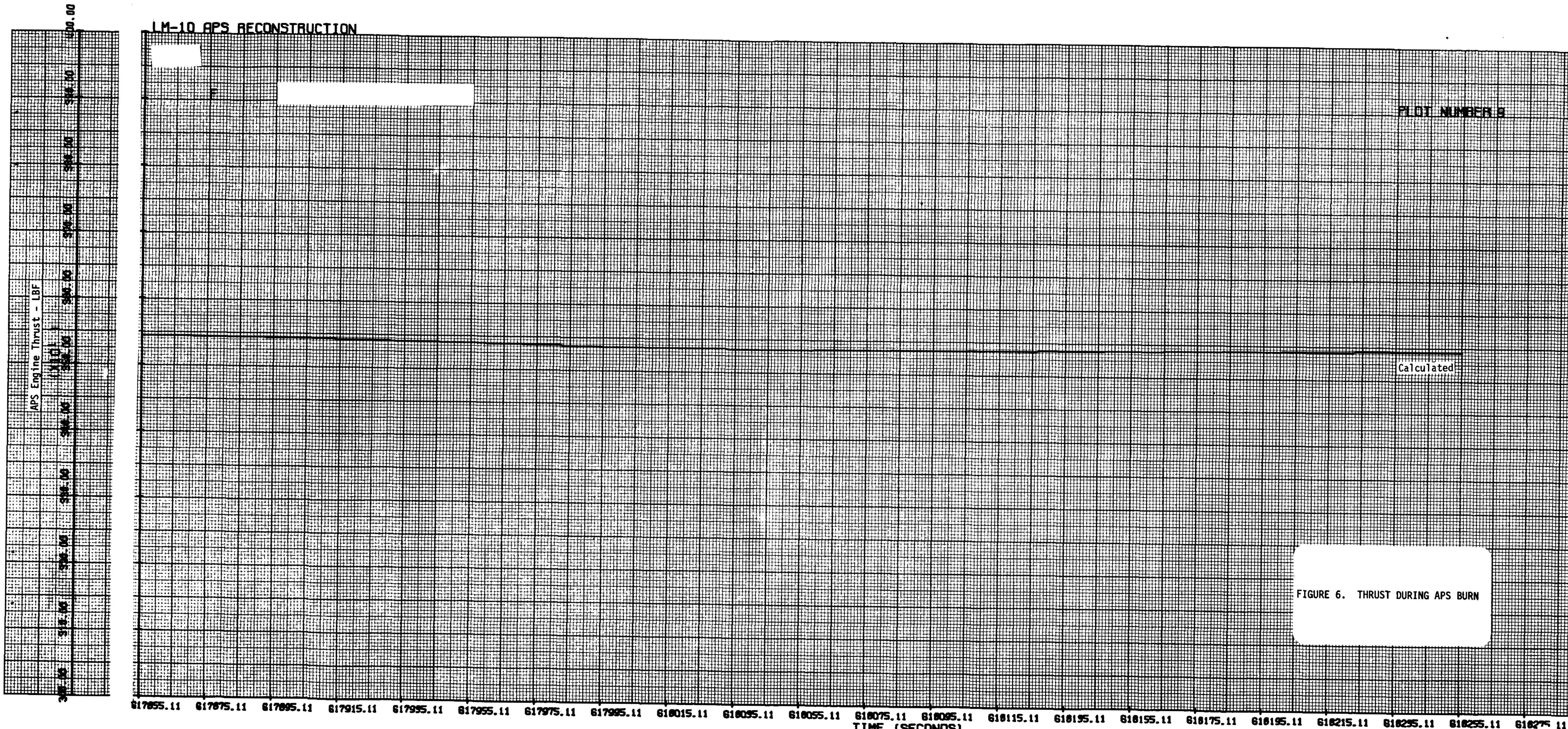


FIGURE 6. THRUST DURING APS BURN

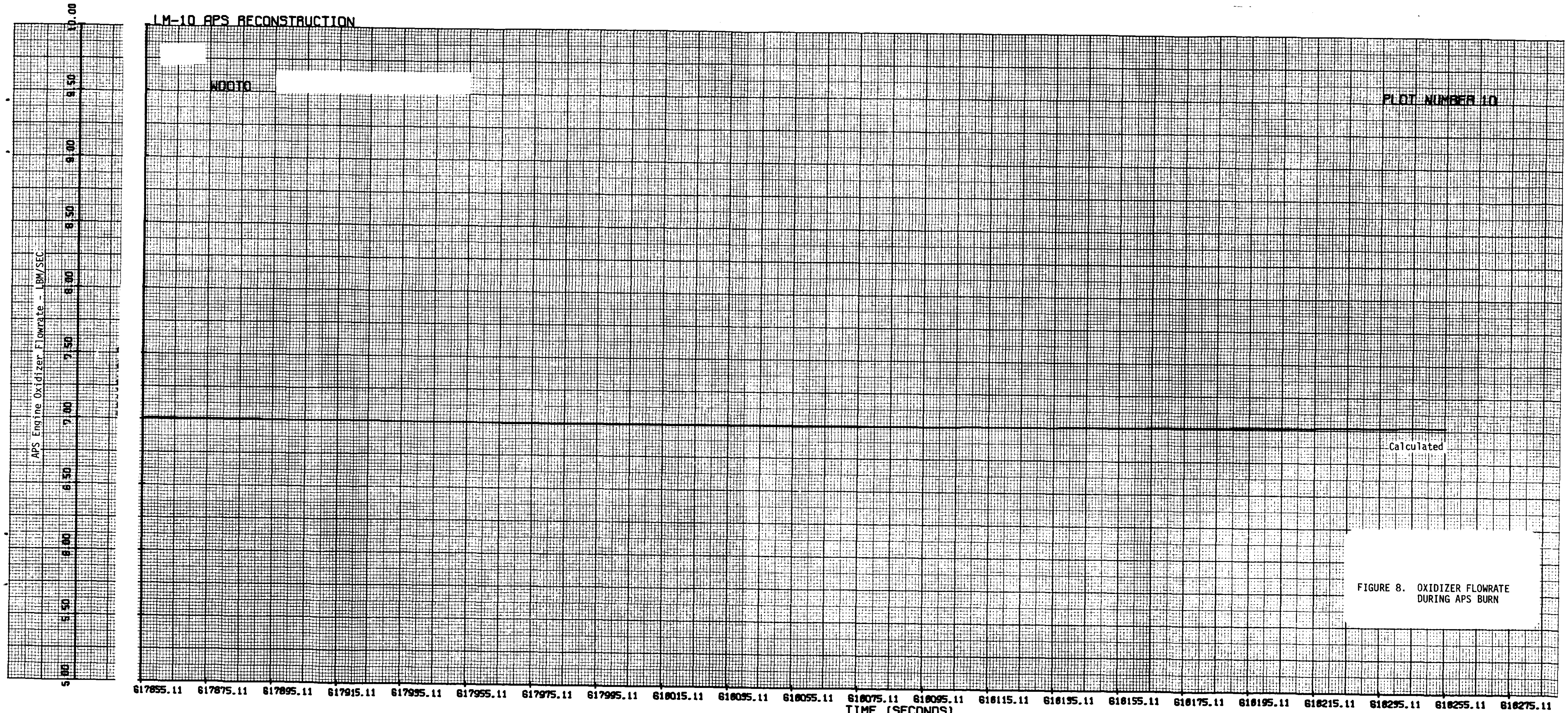


FIGURE 8. OXIDIZER FLOWRATE DURING APS BURN

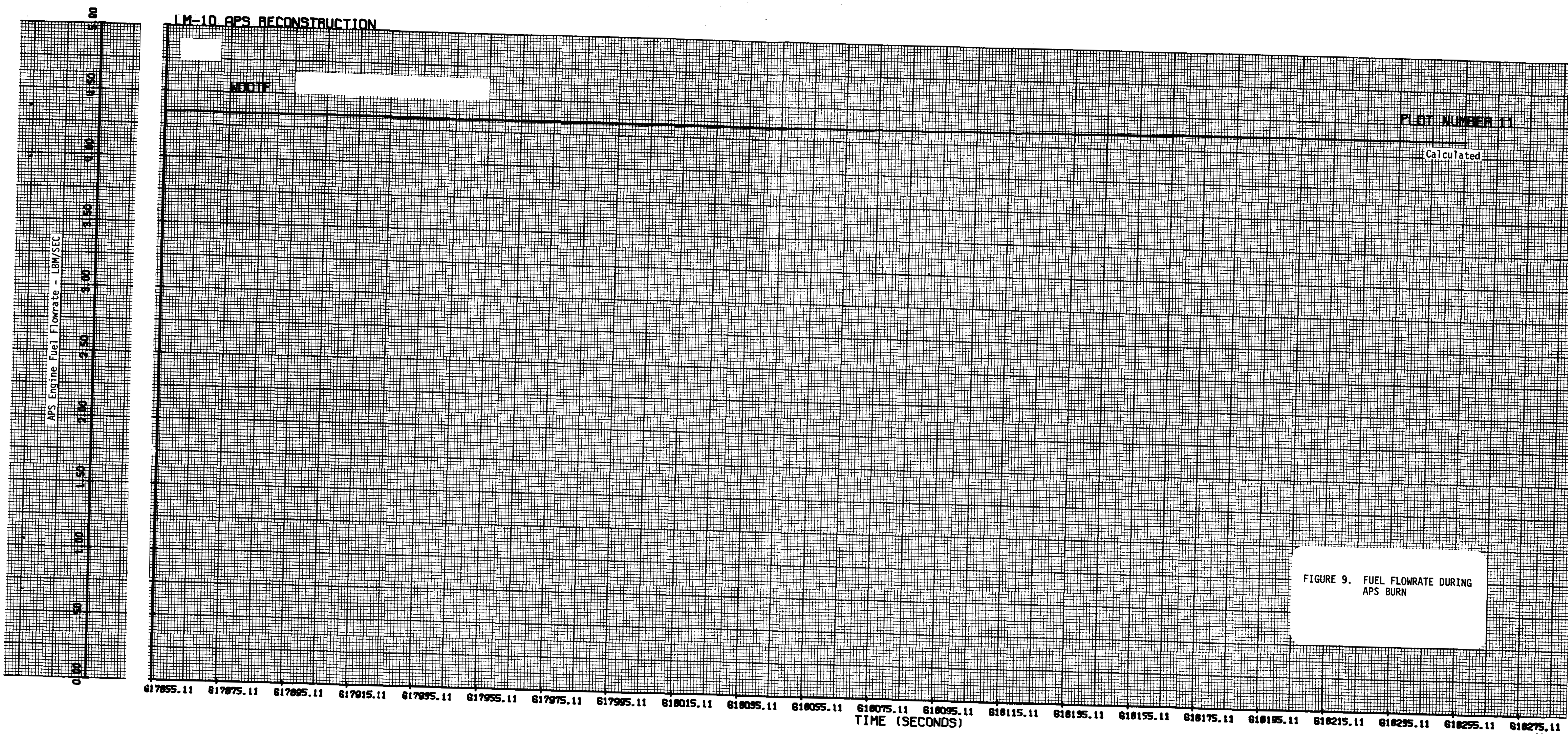


FIGURE 9. FUEL FLOWRATE DURING APS BURN

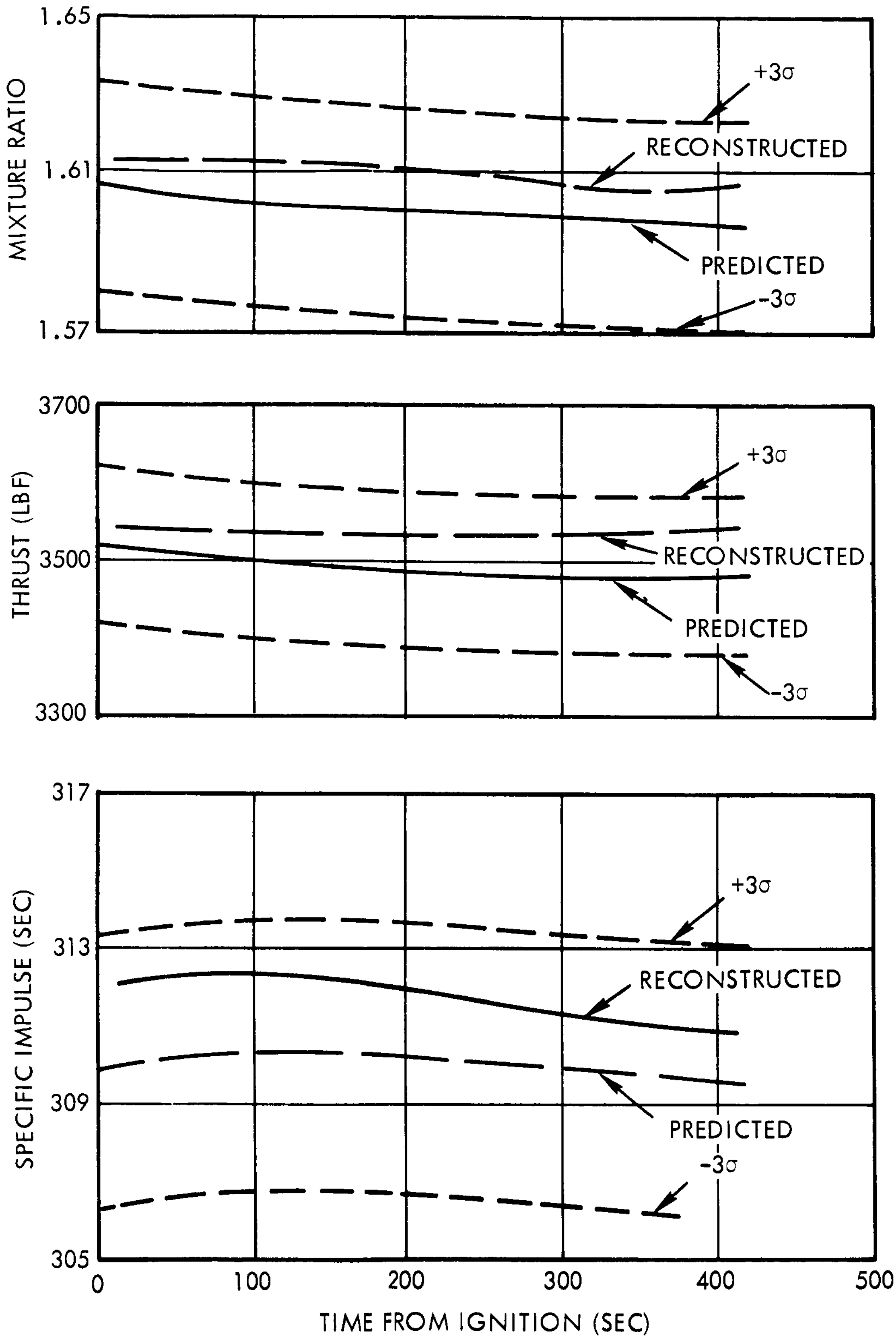


FIGURE 10

COMPARISION OF PREDICTED AND RECONSTRUCTED PERFORMANCE

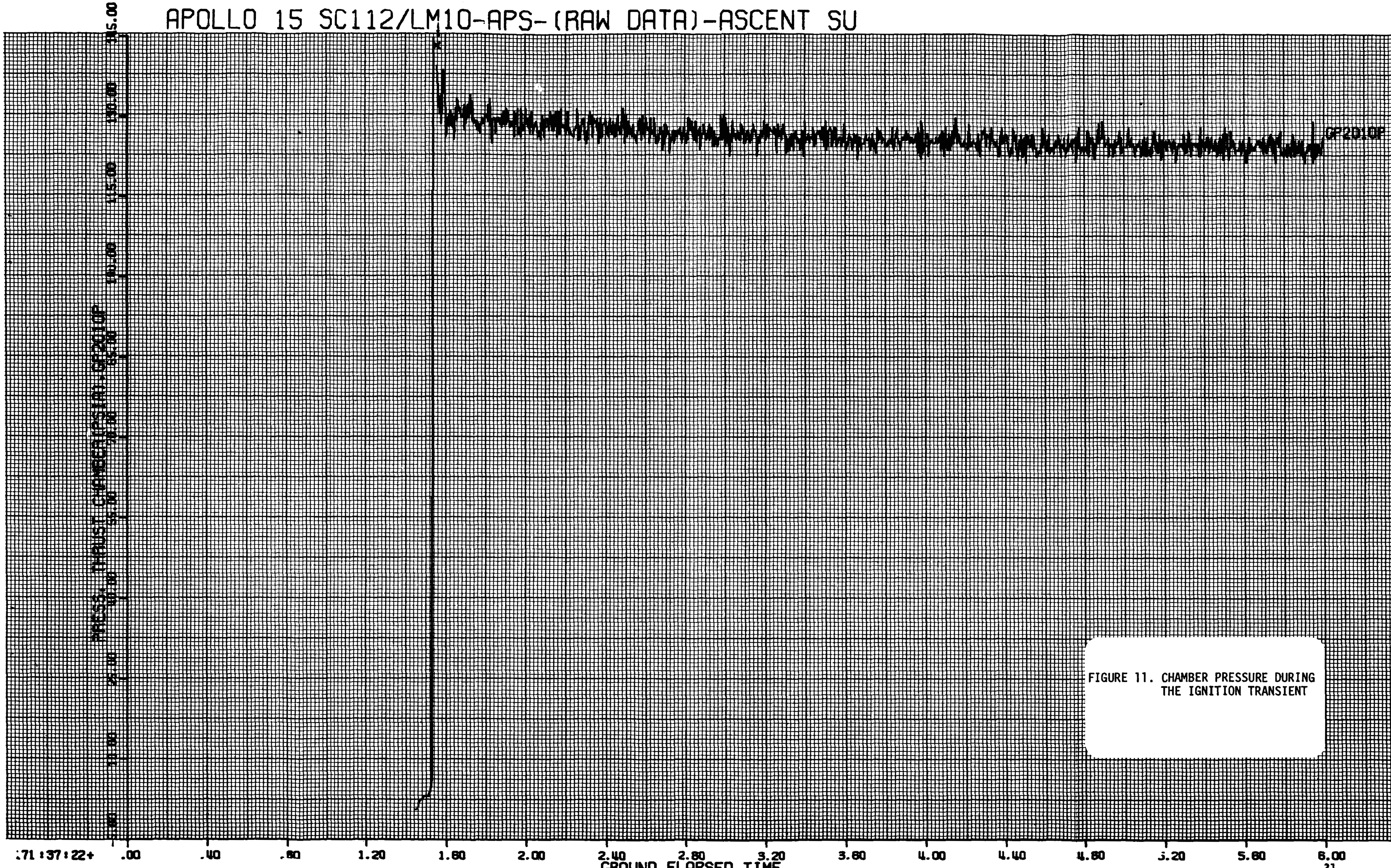


FIGURE 11. CHAMBER PRESSURE DURING THE IGNITION TRANSIENT

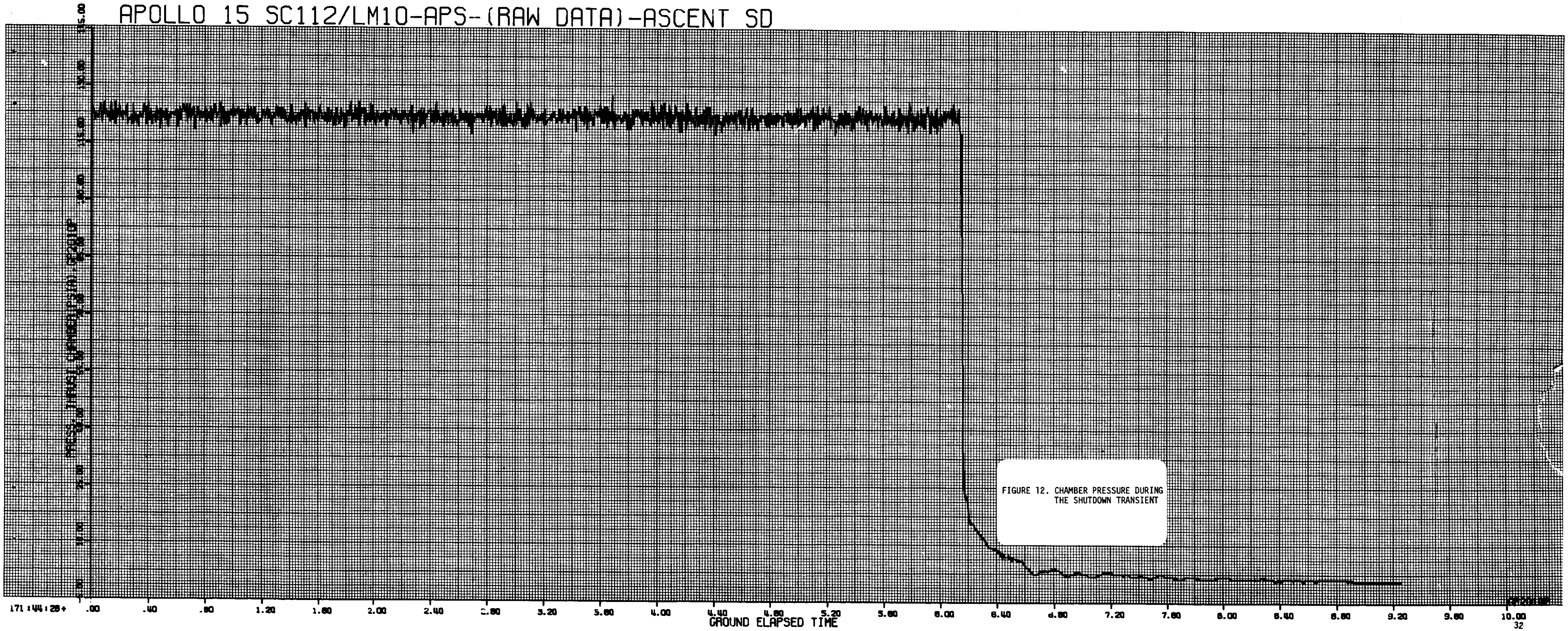


FIGURE 12. CHAMBER PRESSURE DURING THE SHUTDOWN TRANSIENT

APPENDIX

FLIGHT DATA

APOLLO 15 SC112/LM10-APS-(RAW DATA)-ASCENT

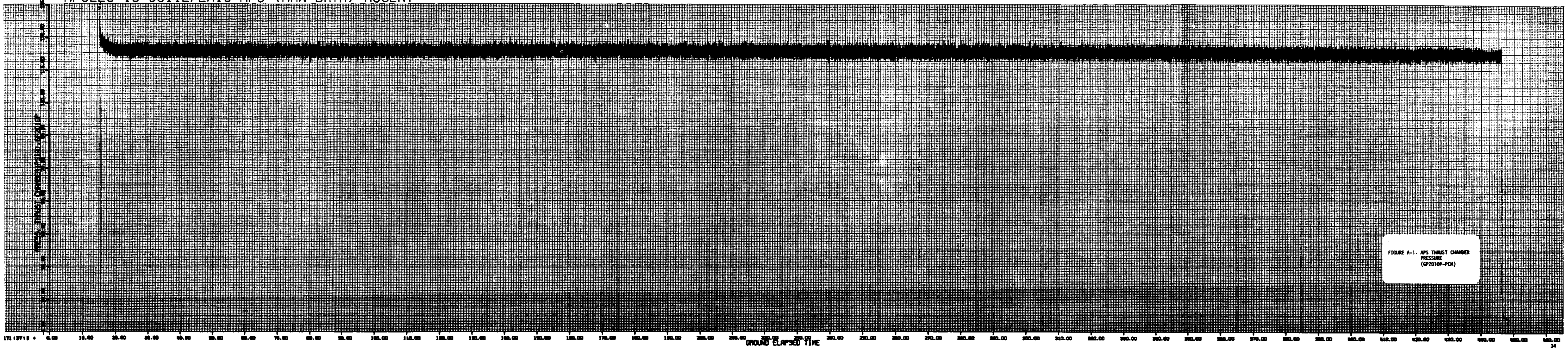


FIGURE A-1. APS THRUST CHAMBER PRESSURE (GP2010P-PCM)

APOLLO 15 SC112/LM10-APS-(RAW DATA)-ASCENT

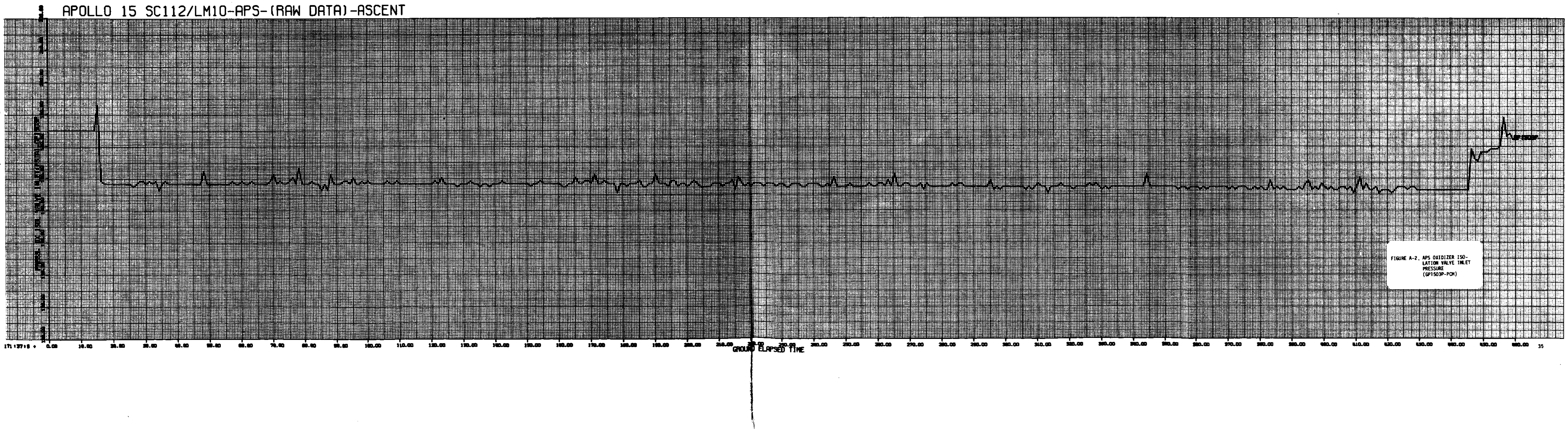


FIGURE A-2. APS OXIDIZER ISOLATION VALVE INLET PRESSURE (GP1503P-PCM)

APOLLO 15 SC112/LM10-APS-(RAW DATA)-ASCENT

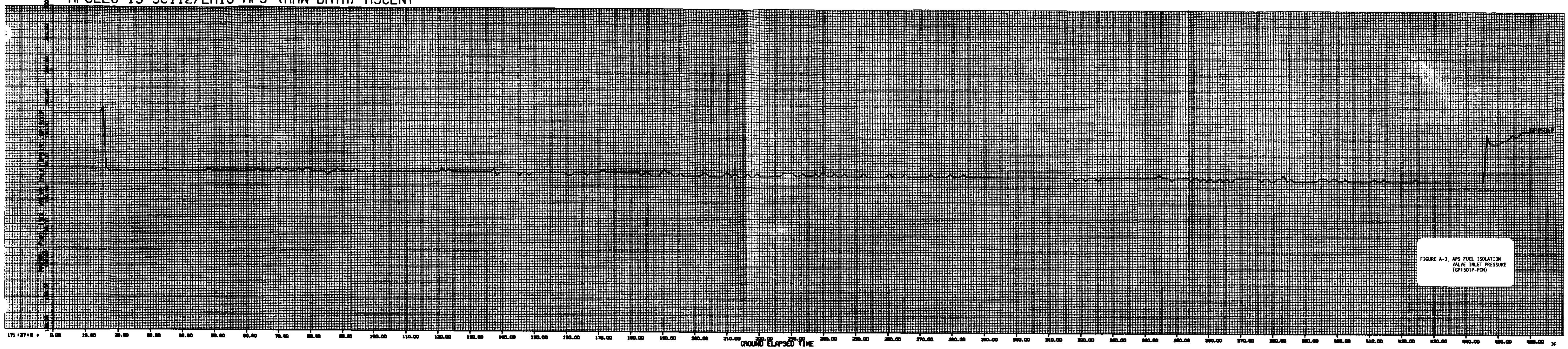


FIGURE A-3. APS FUEL ISOLATION VALVE INLET PRESSURE (GP1501P-PCM)

APOLLO 15 SC112/LM10-APS-(RAW DATA)-ASCENT

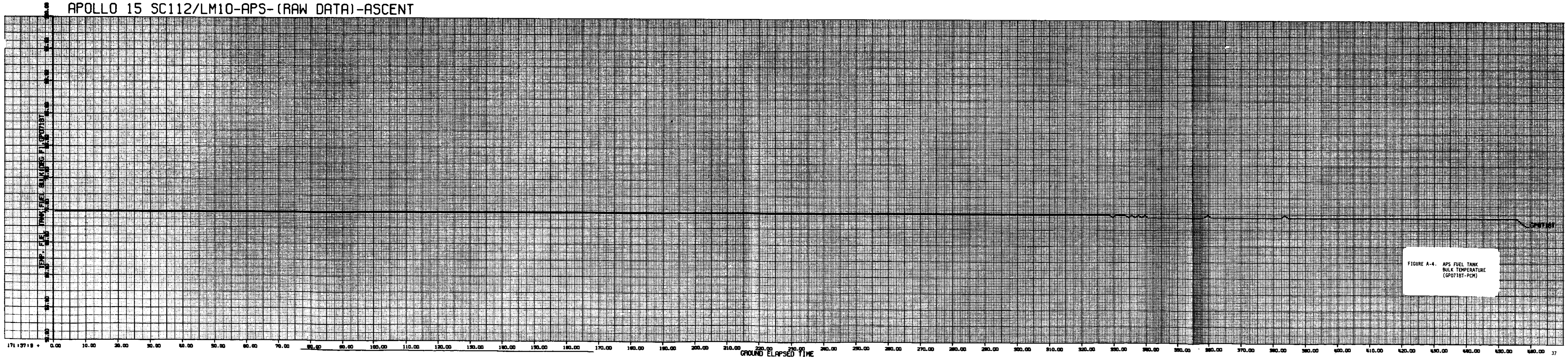


FIGURE A-4. APS FUEL TANK BULK TEMPERATURE (GP0718T-PCM)

APOLLO 15 SC112/LM10-APS-(RAW DATA)-ASCENT

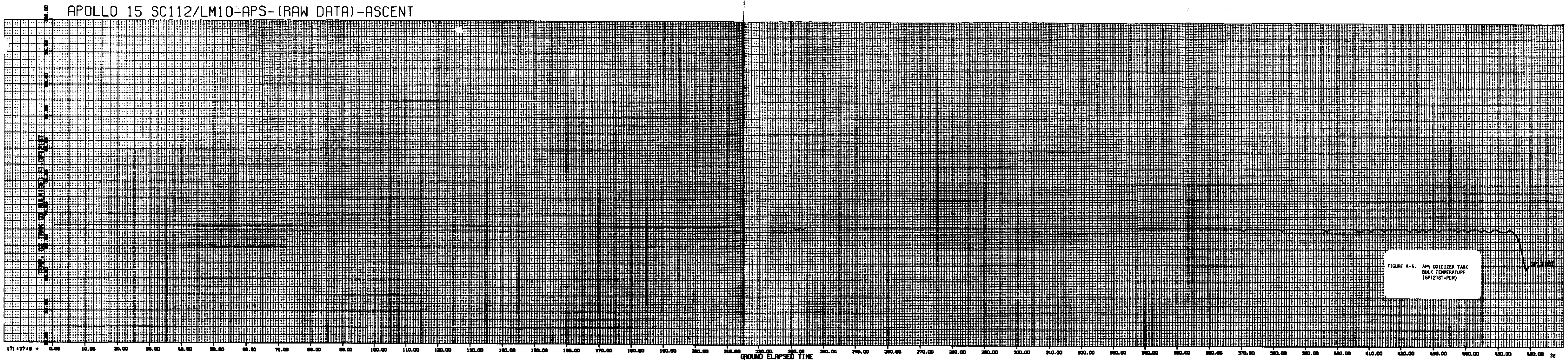


FIGURE A-5. APS OXIDIZER TANK
BULK TEMPERATURE
(GP1218T-PCM)



APOLLO 15 SC112/LM10-APS-(RAW DATA)-ASCENT

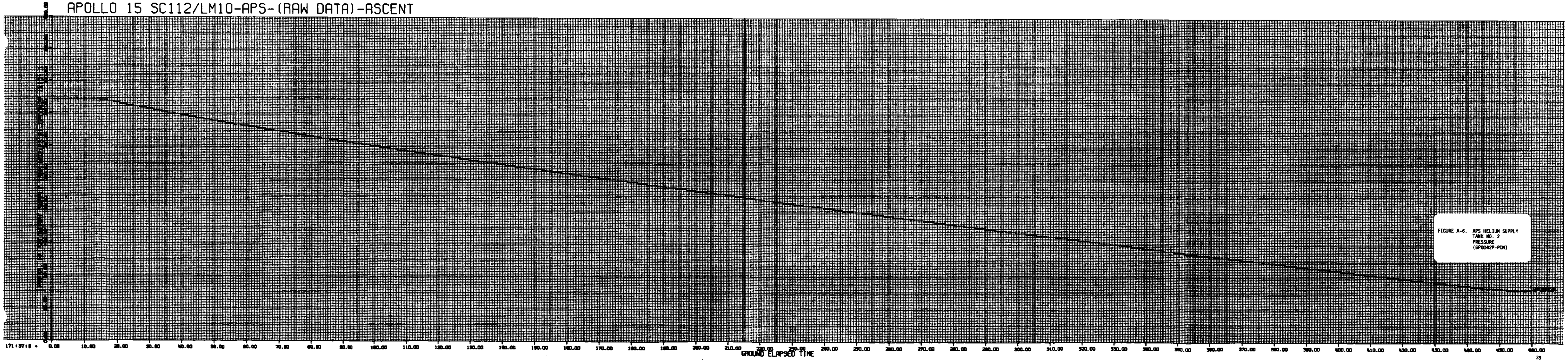


FIGURE A-6. APS HELIUM SUPPLY
TANK NO. 2
PRESSURE
(GP0042P-PCM)

APOLLO 15 SC112/LM10-APS-(RAW DATA)-ASCENT

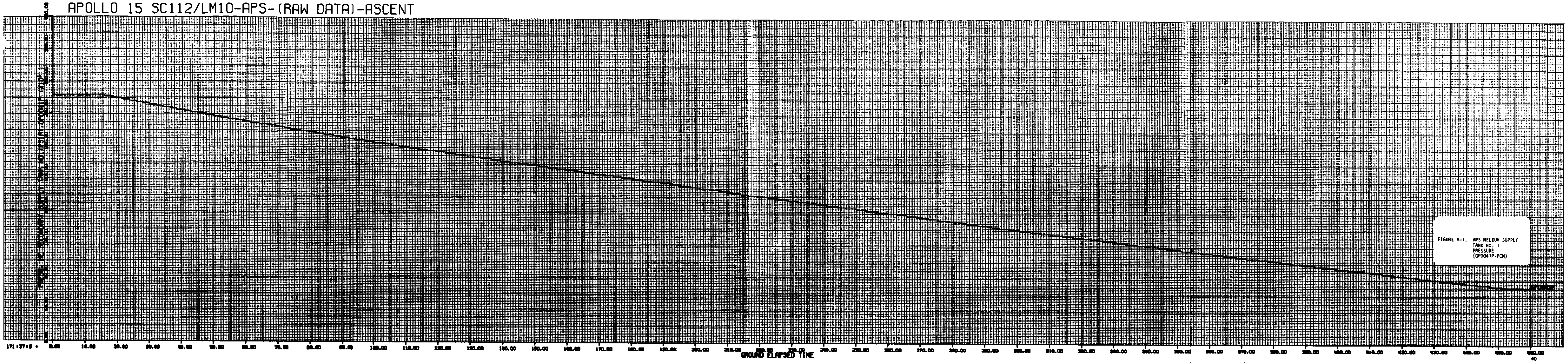


FIGURE A-7. APS HELIUM SUPPLY TANK NO. 1 PRESSURE (GP0041P-PCM)



APOLLO 15 SC112/LM10-APS-(RAW DATA)-ASCENT

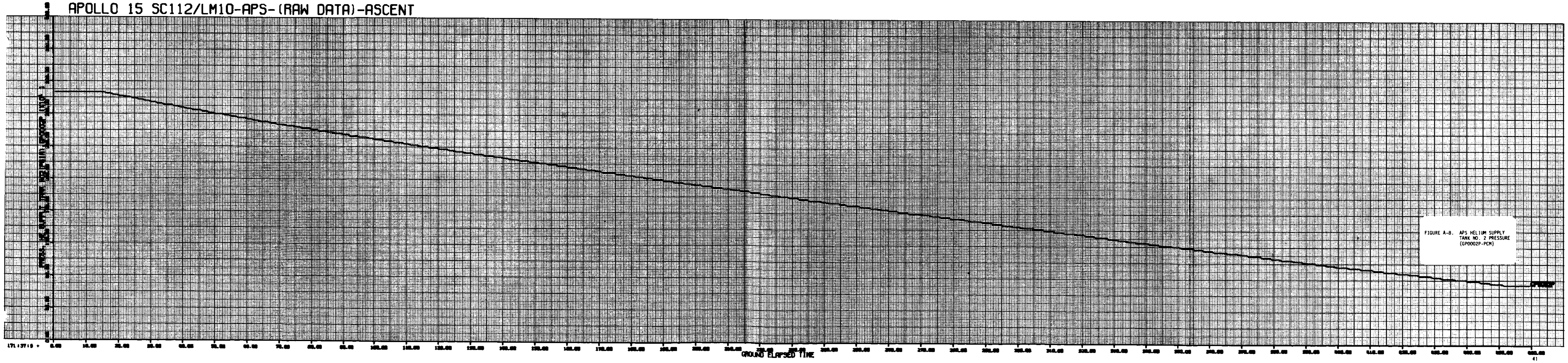


FIGURE A-8. APS HELIUM SUPPLY TANK NO. 2 PRESSURE (GP0002P-PCM)

APOLLO 15 SC112/LM10-APS-(RAW DATA)-ASCENT

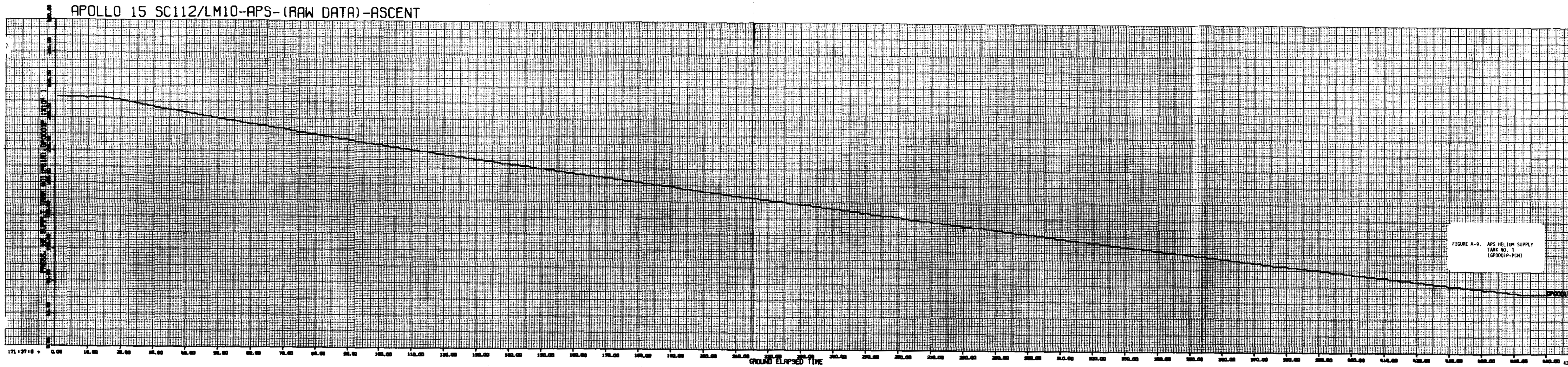


FIGURE A-9. APS HELIUM SUPPLY TANK NO. 1 (GP0001P-PCM)



APOLLO 15 SC112/LM10-APS-(RAW DATA)-ASCENT

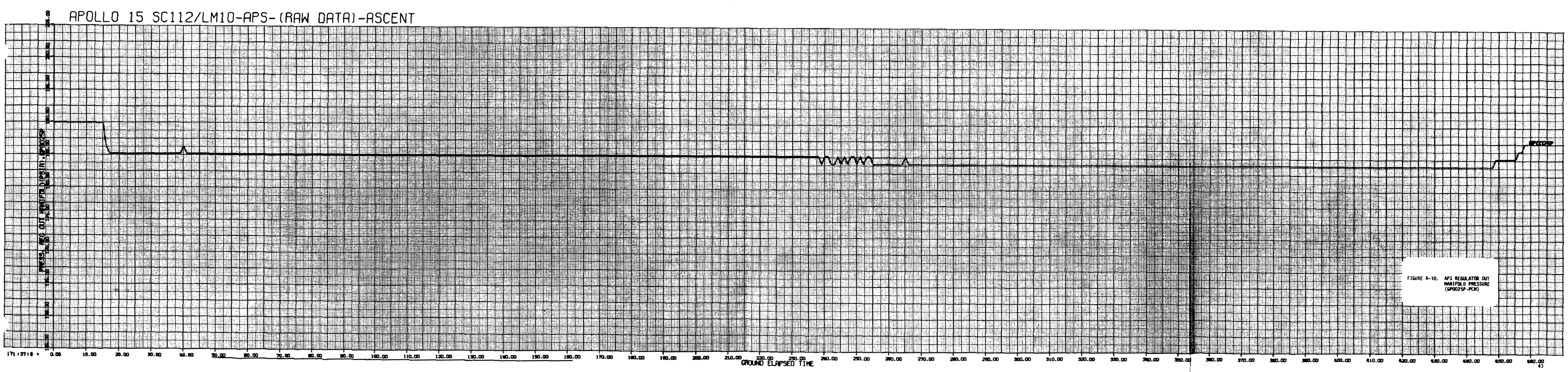


FIGURE A-10. APS REGULATOR OUT MANIFOLD PRESSURE (GP0025P-PCM)

APOLLO 15 SC112/LM10-APS-(RAW DATA)-ASCENT

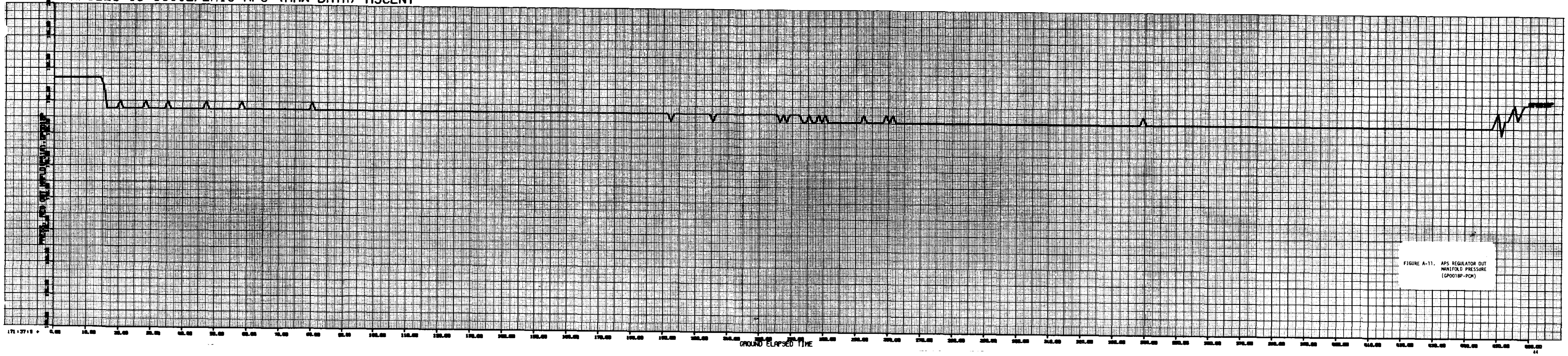


FIGURE A-11. APS REGULATOR OUT MANIFOLD PRESSURE (GP0018P-PCM)